ASME Open Journal of Engineering
Online journal at:
https://asmedigitalcollection.asme.org/openengineering

The Behavior of Vertical Axis Water Turbine With Flexible Blades: Self-Start, Ventilation, and Cavitation

Emine Celik Foust
Department of Civil and Mechanical Engineering,
United States Military Academy,
Mahan Hall, Bldg 752,
West Point, NY 10996
e-mail: foust.emine@westpoint.edu

Three-bladed Darrieus-type vertical axis water turbine is a promising solution for producing electricity with minimal impact on the environment. Although considered a viable option, straight-bladed Darriues-type turbines have not been used commonly due to various operational issues; self-start and stall at low water speeds while ventilation and cavitation are limiting at high water speeds. In this study, the use of flexible blades with an aspect ratio of 2.21 is investigated at water velocities of 0.34, 0.51, 0.68, and 0.85 m/s experimentally. A stiffer turbine that has an 85–95 Shore A hardness blade starts to rotate at 0.51 m/s flow velocity. The more flexible turbine that has a 75–85 Shore A hardness blade starts to rotate at lower water velocities and experiences low rotational speeds resulting in an improved self-start. However, low rotation speed will cause a reduction in the coefficient of performance (C_p). High-speed imaging of the flow field also shows that a low tip speed ratio (TSR) helps to prevent the occurrence of ventilation and cavitation for the turbine with 75–85 Shore A hardness blades. [DOI: 10.1115/1.4063084]

Keywords: hydrokinetic, Darrieus turbine, self-start, cavitation, ventilation, flexible blade, energy harvesting, experimental, fluid flow, power generation, turbines, water

1 Introduction

Harnessing energy by using river turbines can be a reliable solution to produce energy at remote locations. River turbines convert the kinetic energy of flowing rivers into electricity. In these applications, there is no need for building a dam or diverting a river. Because of that, it has a low impact on dissolved oxygen levels, sedimentation, sediment transport, and fish migration. Researchers have investigated several different turbine design concepts in river turbine applications over the years. In general, these turbine designs can be divided into two groups: horizontal-axis and vertical-axis water turbines.

- Horizontal-axis water turbines are the most commonly used type in high-capacity power applications. For example, tidal applications can generate around 1 MW and above. These turbines have a propeller-type rotor with blades. In current applications, horizontal axis turbines are installed either inclined or with their axis of rotation parallel to incoming water flow. Some of the main advantages are improved self-starting and higher values of performance coefficients; C_p of 0.46 at high values of tip speed ratios (TSR of up to 4.5) [1]. While they are one of the most studied types of water turbines, they are still quite expensive to build and maintain. These costs are even more pronounced when the application requires installing submerged generators.
- Vertical-axis water turbines have a simpler construction and design. For this turbine configuration, the axis of rotation is perpendicular to the incoming water flow. In cross-flow applications, the turbine's axis of rotation is parallel but normal to incoming river flow. This type of positioning provides the benefit of installing more turbines in an array configuration and results in higher energy production. In most field applications, generators are installed above the water level in line with the axis of rotation. The advantages of vertical axis water turbines are their simple construction, manufacturability at low cost, and being self-orienting. Drawbacks include the inability to self-start, its low coefficient of performance (C_p values around 0.35 while operating at a TSR of below 3), debris accumulation, shaking, ventilation, and cavitation [2]. The most commonly studied types of vertical axis turbines are Darrieus and Savonius. The main difference between those two designs is the type of force that they use to extract energy. Darrieus-type turbines primarily use lift forces while Savonius type use drag force.

There are several examples of hydrokinetic turbines currently in use. The Smart Monofloat, a three-bladed horizontal axis water turbine with debris protection was installed in the River Inn in Rosenheim, Germany in 2013. In this application, 2 kW of power is produced by a 1 m diameter turbine at 2.1 m/s of incoming flow speed, and the power produced is fed into the grid ([3] Smart Hydro Power[1]). RivGen, a cross-flow helical river turbine

Manuscript received February 2, 2023; final manuscript received July 24, 2023; published online August 17, 2023. Assoc. Editor: Jen-Yuan (James) Chang.

[1]https://www.smart-hydro.de

was deployed on the Kvichak River near Iguigig, AK in 2014. This is a community-scale application and the turbine can generate electricity up to 25 kW at the rated flow speed of 2.25 m/s. The unit has a debris diversion system and can be mounted on a gravity foundation frame [4]. A three-bladed H-Darrieus vertical axis water turbine was installed in the Roza Canal in the US in 2013. Initial testing showed that the 1.5 m height by 3 m diameter turbine can generate 10.9 kW at a flow speed of 2.5 m/s [5].

In this research, a Darrieus-type vertical axis water turbine is studied. As mentioned earlier, some of the drawbacks that limit the application of these turbines are low C_p, negative starting torque, shaking, cavitation, and ventilation. This study aims to investigate the possibility of using flexible turbine blades to improve those issues listed above.

Several research groups focused their attention on improving the performance of the vertical axis river turbines. The US Department of Energy (DOE) conducted performance testing and flow field measurements of a three-bladed horizontal axis turbine (referred to as the Sandia turbine) along with the DOE's reference river turbine. The reference river turbine model consists of a three-bladed Darrieus turbine with NACA 0020 blade profile. This turbine has a 1 m diameter and 1 m height. Three support arms are attached to the blades at half-chord. The experiments performed with the vertical axis Darrieus type reference turbine obtained C_p values of 0.26 at TSR of 1.9 [6].

Reference [7] did a comparative numerical study on how the blade profiles, the number of blades, and water flow velocity affect the turbine torque coefficient and coefficient of performance. Their goal was to come up with a promising hydrokinetic turbine design solution that is easy to manufacture, install and maintain, and suitable for application in the Amazon River. In regards to the number of blades, the use of three and seven blades was compared numerically. Their study recommended the use of seven blades since high solidity provides a higher torque coefficient. In addition, four different blade profiles were investigated including a flat plate configuration, circular arc-shaped blades, NACA 0018, and NACA 1548 profiles. Their computational model results showed that the circular arc profile has the highest torque coefficient around 0.234, resulting in the highest power production [7].

A study published by Ref. [8] investigated the effect of using symmetric and non-symmetric airfoil profiles on the performance of H-Darrieus wind turbines numerically. Their study demonstrated that the S1046 airfoil profile yields the highest coefficient of performance 34.6% ($C_p = 0.346$) for the entire range of TSR. In addition, three wind-lens configurations including flat-panel type, curved surface, and cycloidal surface diffuser have been tested. For all the wind-lens configurations, the presence of wind-lens improves power production over a wide range of TSR. Reference [8] incorporated wind lens since there is a theoretical limit to the amount of energy that can be extracted from wind turbines. This limit is called the Betz limit which has C_p of 0.593. Reference [8] recommended the use of S1046 blade profile with a cycloidal surface wind-lens configuration to obtain a higher coefficient of performance.

The C_p can be optimized by having a duct "diffuser augmentation" around the turbine. Both experimental and numerical studies of ducted three-bladed vertical axis helical river turbines with NACA 63-021 blade profile have been investigated by Ref. [9]. During this study, they compared the results of 2D particle image velocimetry and numerical simulations and obtained similar flow field results from both. The highest coefficient of performance obtained was 45% ($C_p = 0.45$) at 1.9 TSR at the flow speed of 0.3 m/s [9].

In the aforementioned research, the main goal was to improve the performance of the vertical axis water turbine. There are also investigations specifically focusing on improving self-start. In a study performed by Ref. [10], a hybrid turbine consisting of a four-bladed Darrieus turbine with the addition of two-stage Savonius buckets, and a plate deflector were tested experimentally. As an airfoil profile, NACA 0020 was used. Reference [10] installed the Savonius buckets in two ways: at the inside and outside positions above the Darrieus turbine. These configurations were selected to overcome low starting torque. Their results recommended that two-stage Savonius buckets should be installed at a higher position above the Darrieus rotor with a 30 deg angle of a single deflector plate to obtain higher C_p and torque coefficients.

Several studies focused their interest on improving self-start problems on vertical axis turbines by implementing variable pitch control methods. There are two types of variable pitch control methods: passive (self-driven) variable pitch and active (forced) variable pitch. Passive variable pitch refers to methods that do not require a control system with sensors, microprocessors, and stepper motors. In a passive variable pitch system, aerodynamic forces generated on the blades actuate the pitching motion of the blades. An example of a passive method is using pins as stoppers to limit the pitch angle of Darrieus blades as presented in a study by Ref. [11]. These stoppers limit the tail of the airfoil to move between −20 deg and 20 deg [11]. In a separate study performed by Ref. [12], the variable pitch of turbine blades was achieved by attaching two balancing masses to each blade. The type of turbine used in that study is a vertical axis cross-flow Darrieus type tidal current turbine referred to as the KOBOLD turbine. In this unique method, turbine blades move to their ideal position due to a change in the center of gravity.

The active (forced) variable pitch control method uses sensors and external control mechanisms to change the pitch angle of the turbine blade. Examples of this method are Pinson cycloturbine, gears and sprockets, and cam-driven actuators. Reference [13] tested two small cross-flow hydrokinetic turbines. One with sinusoidal pitch obtained by an eccentric ring attached to control arms and the second one with cam-driven variable pitch capability. In a cam-driven control system, a central cam and pushrods control the pitch of each blade. Two-dimensional modeling results show a peak C_p of 0.45 for sinusoidal pitching with a passive eccentric ring system and around C_p of 0.49 for the cam-driven active control system. However, experimental results show C_p values below 0.32 for both systems due to parasitic losses and small turbine model size [13].

The application of a flexible airfoil on Darrieus type straight-bladed vertical axis wind turbine has been studied numerically as one of the passive control methods by Ref. [14]. This study mainly focused on the structural analysis of a single turbine blade regarding bending and twisting motion at various TSR values. An increase in the TSR resulted in an upsurge in peak values of bending and twist deformation. In a combined experimental and numerical study performed by Ref. [15], they used a turbine blade with chordwise flexibility. That study illustrated that the performance of the flexible airfoil in wind turbine application improves at low tip speed ratios but C_p decreases at high TSR. Both of these studies mainly focused on wind turbine applications. There is still a need for further study to investigate the influence of blade flexibility on vertical axis water turbines as water turbines experience different issues associated with turbine operation due to free surface interaction. In this study, the goal is to investigate the effect of turbine blade flexibility (both spanwise and chordwise) for a vertical axis water turbine on self-start, ventilation, and cavitation experimentally.

2 Materials and Methods

There are several factors to consider when designing a vertical-axis water turbine. For this study, a three-bladed Darrieus turbine with a rotor solidity of 1.63 is used. The solidity of a turbine is defined as the ratio of total blade area to disk area. There are several methods available in the literature to calculate solidity. In this study, it is calculated as

$$\frac{NC}{R} \tag{1}$$

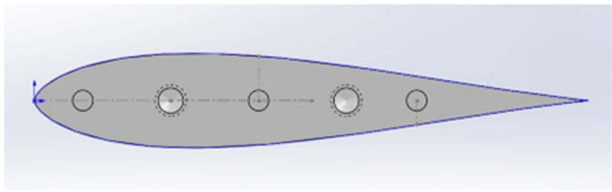

Fig. 1 SOLIDWORKS part drawing of S1046 airfoil profile

In Eq. (1), C is the chord length, N is the number of blades, and R is the radius of the rotor.

The airfoil profile of S1046 is used due to its high coefficient of performance. As shown in Fig. 1, the S1046 airfoil has a symmetrical profile. Reference [8] numerically assessed the aerodynamic performance of 24 airfoil profiles both symmetric and non-symmetric. They concluded that symmetric S1046 is the best-performing airfoil profile in the range of 2–7 TSR.

Another important factor in turbine design is the aspect ratio (AR), defined as the ratio of the blade length (H) to the rotor radius (R). For this study, two aspect ratios were tested: AR_1 of 2.21 and AR_2 of 1.47. In Table 1, the important design parameters of the Darrieus turbine are summarized.

All the measurements are performed in a water channel. The test section is 2440 mm long, 152.4 mm deep, and 152.4 mm wide. A centrifugal pump with variable speed control is used to provide a wide range of inflow water speeds ranging from 0.061 m/s to 1.73 m/s. Laser Doppler velocimetry technique is employed, to determine flow velocities and to calibrate the water channel. An overview of the experimental system along with instrumentation is shown in Fig. 2. It should be noted that the turbine is located in a small channel that provides stream-tube confinement.

For the first part of the study, turbine blades that are made out of acrylonitrile butadiene styrene (ABS) are used. Blades are 3D printed with the support arms attached. The rest of the system components including the turbine shaft and clamps are custom-made in the machine shop from stainless steel. To evaluate the performance of the turbine, two dimensionless numbers are calculated: C_p and TSR. Vernier force sensor and Vernier rotary motion sensors are utilized along with the LABVIEW data acquisition system to perform measurements of force and angular velocity. Figure 2 shows the turbine model with the sensors attached. The rotary encoder measures angular position at a sampling period of 0.1 s, which could then be converted to angular velocity through MATLAB code. The torque is calculated by multiplying the force measurements from the Vernier sensor with the moment arm length, which is 50 mm long. After determining torque and angular velocity, the C_p can be calculated by using the following equations:

$$C_p = \frac{\text{Power extracted}}{\text{Power available}} \tag{2}$$

$$\text{Power extracted} = \text{Torque} \times \text{Angular velocity} \tag{3}$$

$$\text{Power available} = \frac{1}{2}\rho A U^3 \tag{4}$$

Table 1 Design parameters of the Darrieus turbine used in this study

Definition	Details
Blade height (H)	102 mm
Chord length (C)	25 mm
Number of blades (N)	3
Turbine radius (R)	46 mm
Solidity (σ)	1.63
Blade profile	S1046

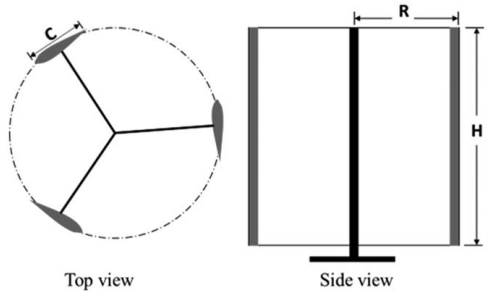

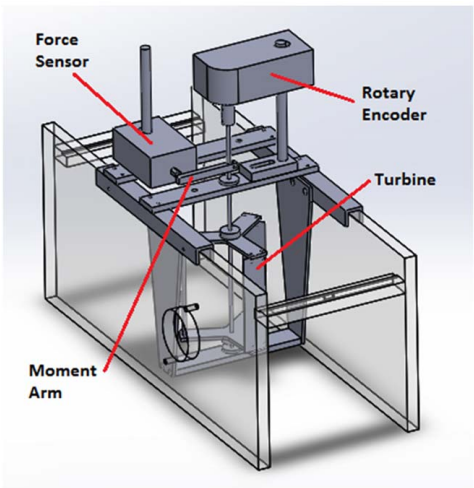

Fig. 2 Experimental setup in the water channel

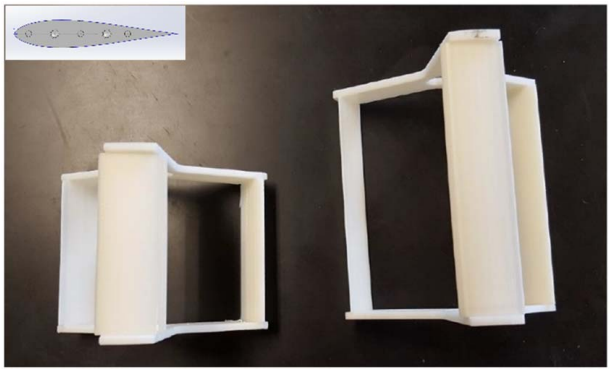

Fig. 3 3D printed Darrieus turbines with aspect ratio of 1.47 on the left side and 2.21 on the right image

In Eq. (4), ρ is the density of water and is assumed to be 1000 kg/m^3, U is the velocity of water, and A is the swept area of the turbine. For a Darrieus turbine, the swept area is calculated as turbine blade height (H) multiplied by turbine diameter ($2R$).

In the second part of the study, the use of flexible blades for the AR that provided the highest C_p is investigated. In the case of flexible hydrofoil, turbine blades are made out of thermoplastic polyurethane (TPU). For additive manufacturing, the Prusa I3 MK3S 3D printer is used since it is very difficult to print TPU on standard machines. One of the common issues is that the filament kinks up and wraps around the extruder in a traditional 3D printer. Prusa I3 MK3S 3D printer is designed in a way that eliminates these issues.

For the experiments, two different blade hardness values were desired: 75–85 Shore A and 85–95 Shore A hardness range. During 3D printing, several parameters were varied to obtain desired surface quality and hardness values. These parameters are printing material, printing orientation (horizontal versus vertical), blade design, and infill amount. After several testing, it was determined that the infill amount influences the flexibility of the blades the most. A 75% infill resulted in 85–95 Shore A blade hardness while a 50% infill provided in 75–85 Shore A hardness. Details of flexible airfoil manufacturing methods are explained more in detail by Ref. [16]. Flow visualization images are captured by a high-speed camera with a frame rate of 60 frames/s.

3 Results and Discussions

3.1 Influence of the Aspect Ratio on Turbine Performance. In the first part of the study, the effect of aspect ratio on turbine performance is investigated for a three-bladed Darrieus turbine when the blades are made out of ABS. The aspect ratios tested in the water channel are $AR_1 = 2.21$ and $AR_2 = 1.47$. It is important to note that the turbine radius values are identical and the height of the turbine is varied to change the aspect ratio.

Both turbines are 3D printed with the support arms attached at the blade ends as shown in Fig. 3. During preliminary testing, it was observed that at flow velocities above 0.85 m/s, there is water spillage from the tank and the formation of surface waves. Force and angular velocity measurements are performed at a flow velocity of 0.85 m/s. The Reynolds number corresponding to a water velocity of 0.85 m/s is 2.54×10^6. The chord length of the S1046 airfoil profile is used as the characteristic length in the Reynolds number equation. Table 2 summarizes the results of water channel testing at a flow velocity of 0.85 m/s.

During testing, average rotational velocities are calculated as 286 rpm and 208 rpm for $AR_1 = 2.21$ and $AR_2 = 1.47$ correspondingly. The reduction in rotational velocity will cause the TSR to be 27% lower for $AR_2 = 1.47$. The C_p values are calculated from torque and rotational velocity measurements in the test channel. The average C_p values are 0.025 and 0.019 for $AR_1 = 2.21$ and $AR_2 = 1.47$. To conclude, increasing the aspect ratio resulted in a higher coefficient of performance C_p. For the turbine with flexible blades, the aspect ratio of 2.21 is used.

3.2 Influence of Having Flexible Turbine Blades on Turbine Performance. Several methods including molding, 3D printing, and machining were explored to manufacture flexible turbine blades. Among all the methods considered, 3D printing the turbine blades out of TPU provided the best surface quality. The printer used for additive manufacturing is the Prusa I3 MK3S 3D printer. This printer is capable of handling flexible filaments such as thermoplastic elastomer and TPU. TPU is used in this study since it offers flexibility and solidity at the same time and has a hardness range of 60–90 Shore A. Two different hardness values were tested for the turbine blades: 75–85 Shore A and 85–95 Shore A hardness. Unlike the turbine made out of ABS, support structures holding support arms are 3D printed separately. Flexible turbine blades are attached to two rigid support structures at blade ends. It is important to note that there is no metal stiffener in the blades. Blades have both spanwise and chordwise flexibility.

Observations from high-speed imaging of two Darrieus turbines, one with blade hardness of 75–85 Shore A and the second one with 85–95 Shore A are summarized in Table 3. Several visuals were performed at various water velocities of 0.34, 0.51, 0.68, and 0.85 m/s. The rotational speed and TSR values were calculated from the recorded videos after the turbine started to rotate. At a water velocity of 0.34 m/s, a turbine with 75–85 Shore A blade hardness rotates freely while a turbine with a blade hardness of 85–95 Shore A does not rotate. At 0.51 m/s flow velocity, both turbines rotate freely, and as water velocity increases, their rotational speed increases. It is also shown that although a turbine with 75–85 Shore A blades starts to rotate at lower water velocities, it experiences lower rotation speed in comparison with an 85–95 Shore A turbine at all flow speeds. The percentage differences in rotation speeds are 70%, 67%, and 64% at $U = 0.51$, 0.68, and 0.85 m/s, respectively.

It is essential to highlight that flow velocities below 0.34 m/s were included in the testing protocol. However, it is noteworthy that the data points obtained at these low velocities were ultimately excluded from the study's analysis. The rationale behind this exclusion was the absence of rotational movement observed in both turbines under such conditions. In addition, corresponding TSR values are listed in Table 3. Low flow speed results in lower TSR for 75–85 Shore A hardness turbine as shown in Fig. 4. The earlier numerical study performed by Ref. [16] for an ABS turbine showed that lowering TSR will reduce the C_p. Thus, it can be concluded that increasing blade flexibility improves the self-start problem while providing less power due to reduced TSR for the same water

Table 2 Summary of experimental results including average rotational velocity, TSR, and C_p corresponding to $AR_1 = 2.21$ and $AR_2 = 1.47$

Flow velocity (m/s)	Turbine radius (mm)	Chord length (mm)	Blade height (mm)	AR	Average rotational velocity (rpm)	Average TSR	Average C_p
0.85	46	25	102	2.21	286	1.62	0.025
0.85	46	25	68	1.47	205	1.16	0.019

Table 3 Water velocity and rotational speed values of turbines that have 3D printed blades made from TPU with 85–95 Shore A and 75–85 Shore A

Flow velocity (m/s)	Turbine blade type	Rotational speed (rpm)	TSR
0.34	75A–85A TPU	16	0.23
	85A–95A TPU	0	0.00
0.51	75A–85A TPU	54	0.51
	85A–95A TPU	180	1.70
0.68	75A–85A TPU	88	0.62
	85A–95A TPU	264	1.87
0.85	75A–85A TPU	112	0.63
	85A–95A TPU	308	1.75

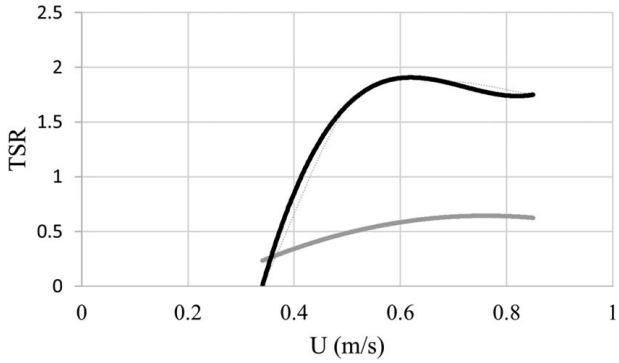

Fig. 4 Effect of blade flexibility on TSR

velocity values. To understand the reduction in TSR, the deflection behavior of the blades is analyzed in Figs. 5 and 6. Figure 5 depicts the instantaneous images of the turbine with 75–85 Shore A hardness blades when the water velocity is 0.34, 0.51, 0.68, and 0.85 m/s. As shown in Table 3, the flexible turbine is rotating at all flow speeds. For 0.34 m/s, flexible blades do not experience any noticeable deflection. As flow velocity increases, the amount of spanwise blade deflection in the opposite direction of centrifugal force is getting larger. The maximum deflection region occurs in the middle portion of the blades since the blades are attached to the support structure at the blade ends. For a flow velocity of 0.85 m/s, the deflection region is shown in the figure with an arrow. Figure 6 examines the operation of the turbine with an 85–95 Shore A hardness blade corresponding to a less flexible blade. Note that at 0.34 m/s, the less flexible turbine is not rotating and there is no noticeable deflection. As water velocity increases, there is some visible deflection but still not as pronounced as in the case of the flexible blades. At 0.85 m/s, there is deflection and twist of the blades. It has also been observed that high TSR values lead to more complicated bending and twisting of the turbine blades.

In addition to the self-start problem, turbine operation is analyzed in regard to the occurrence of ventilation and cavitation. Ventilation is associated with the entrainment of air bubbles to the turbine from the free surface while cavitation refers to the formation of water vapor in regions of low pressure. Earlier studies have shown that local high-water velocities could cause local pressure to drop below vapor pressure and cause cavitation bubbles to form [2]. Both cavitation and ventilation have been known to harm turbine performance and should be avoided.

In Fig. 7, six-time instances of the flexible blade turbine operation at the flow velocity of 0.68 m/s are shown. It should be noted that for this flow velocity, the turbine is rotating at 88 rpm. Although there is a development of a small-scale surface wave, there is no noticeable sign of ventilation or cavitation.

In Fig. 8, six-time instances during the operation of the turbine with the less flexible (85–95 Shore A hardness) blades at a water speed of 0.68 m/s are illustrated. At various time instances such as at $t = 1.6$ s, 6.4 s, and 12.8 s, the development of a large bubble at the top portion of the blade and along the support arm is observed. At this flow speed, the turbine is rotating at 264 rpm. High rotation speed causes the formation of a free surface wave and the entrainment of air bubbles. This phenomenon is known as ventilation. This behavior is mainly observed at a TSR of 1.87, corresponding to $U = 0.68$ m/s. For the less flexible blade turbine when the flow speed is increased to $U = 0.85$ m/s, the rotation speed of the turbine becomes 308 rpm, which corresponds to a TSR of 1.75. In that case, the formation of the free surface wave is still observed but the entrainment of air bubbles from the top is rare as shown in Fig. 9. This figure shows two-time instances at which there are noticeable bubbles. This can be explained by the increase in wave height upstream and the reduction in water height downstream. This results in the turbine shaft being completely submerged compared to Fig. 8. In Fig. 9, bubble entrapment is mainly due to free surface waves crashing further downstream and introducing bubbles into the turbine. For flow speeds of 0.85 m/s, this behavior

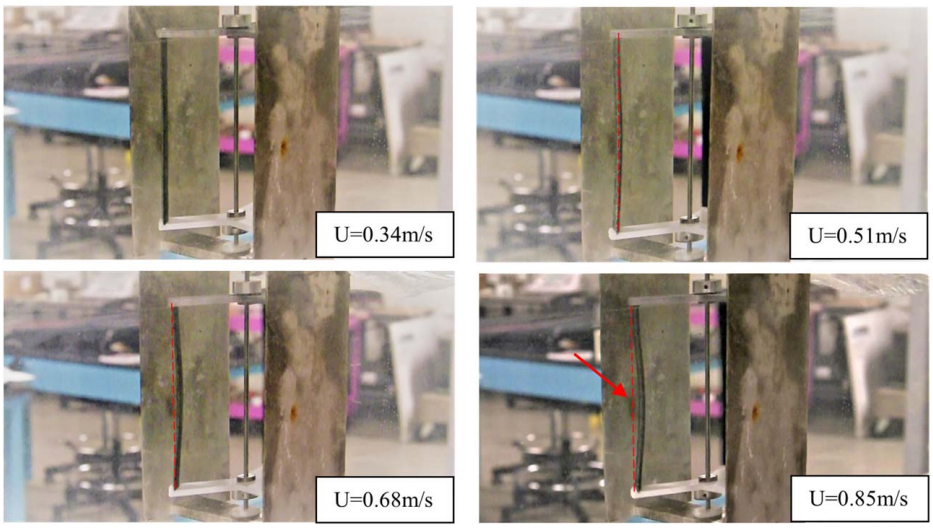

Fig. 5 75–85 Shore A hardness blade during operation at water velocity values ranging from 0.34 m/s to 0.85 m/s

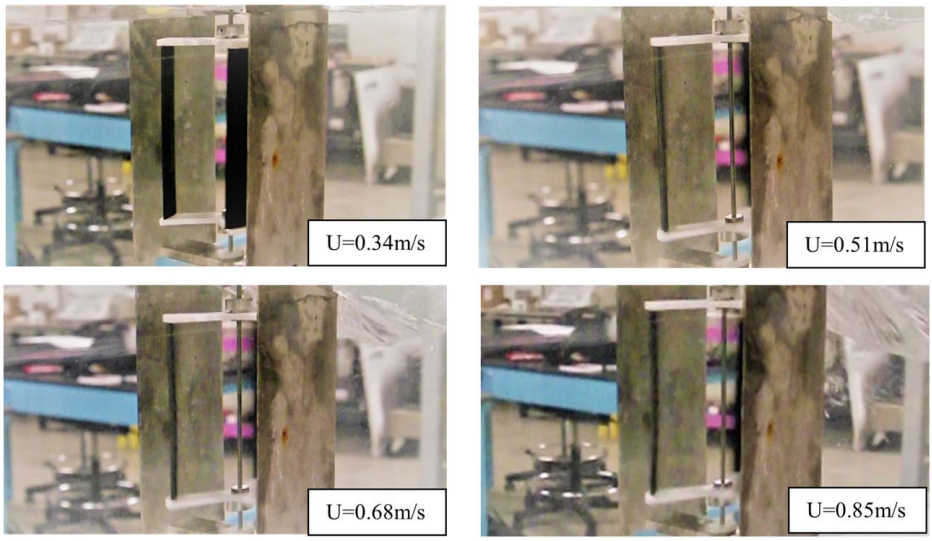

Fig. 6 85–95 Shore A hardness blade during operation at water velocity values ranging from 0.34 m/s to 0.85 m/s

Fig. 7 Instantaneous images of flexible (75–85 Shore A hardness) blade turbine at a flow speed of 0.68 m/s while operating

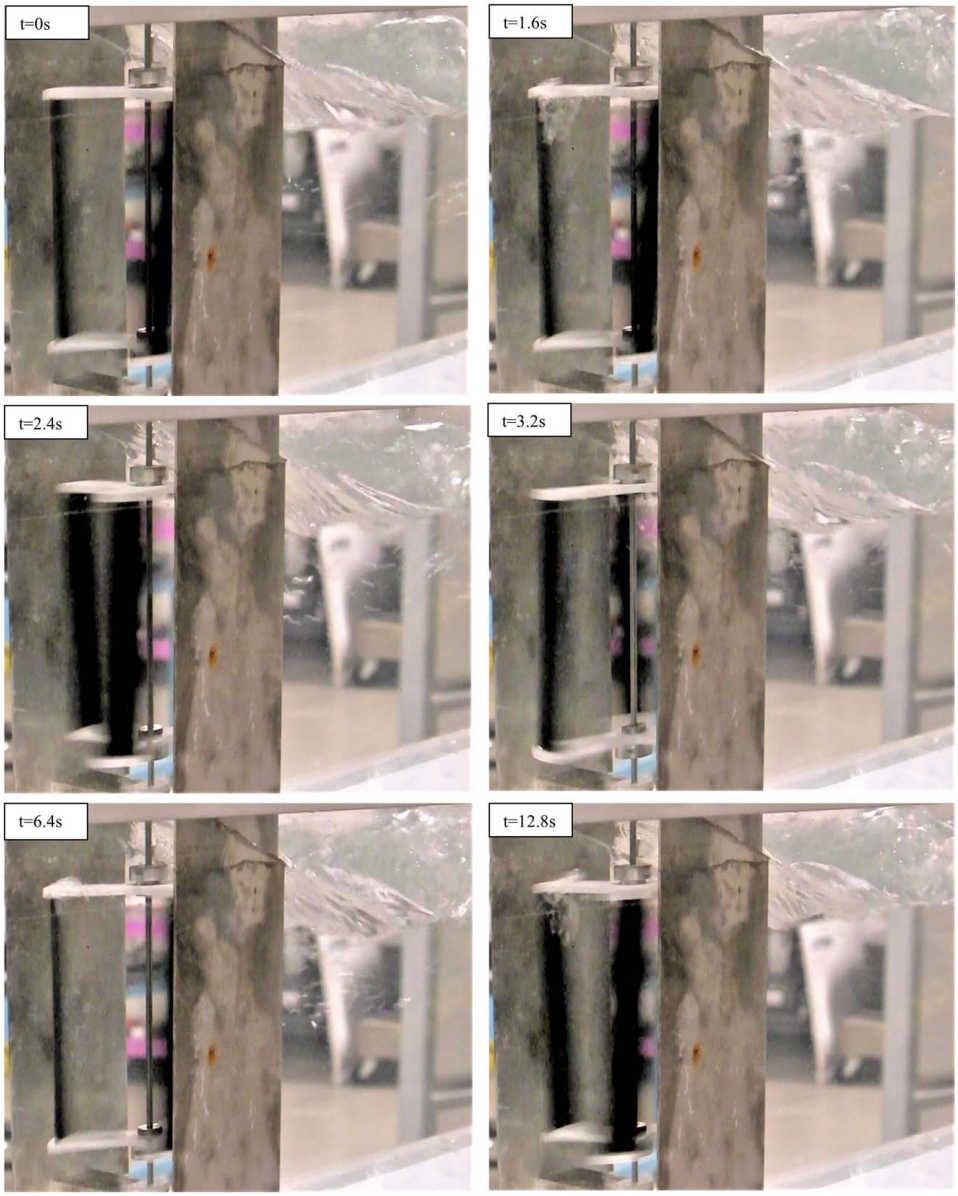

Fig. 8 Images of a less flexible (85–95 Shore A hardness) blade turbine at 0.68 m/s flow speed while operating

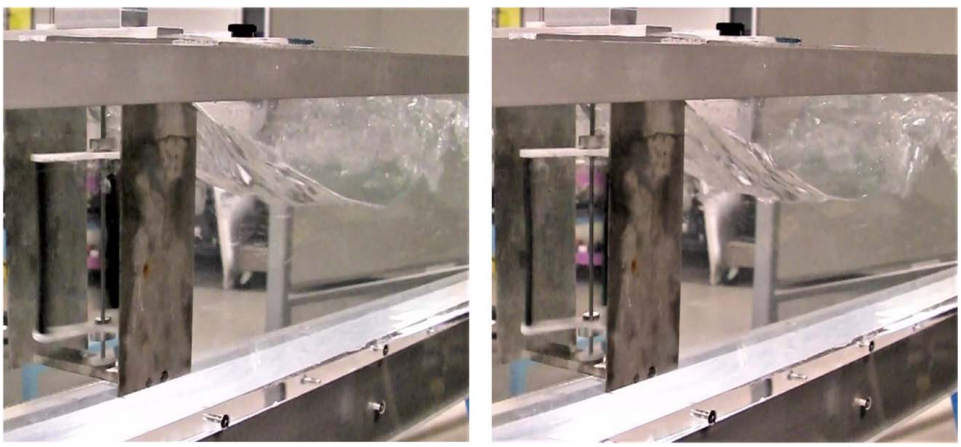

Fig. 9 Flow imaging of a turbine with 85–95 Shore A hardness turbine at two-time instances when the flow velocity is 0.85 m/s

could be associated with both ventilation and cavitation. To prevent ventilation, the turbine should be located away from the free surface. In terms of cavitation, reducing rotation speed (lower local velocities) and avoiding the channeling effect should improve that issue. It should be noted that the 75–85 Shore A turbine did not experience cavitation or ventilation even at the highest flow velocity of 0.85 m/s. This could be associated with the low TSR operation due to blade deflection.

4 Conclusions

Fixed-pitch Darrieus turbines are known to experience self-start, ventilation, and cavitation problems during operation. The effect of using flexible turbine blades to improve these problems has been investigated in this study. Two turbines have been built; one with blade hardness of 75–85 Shore A and the second one with 85–95 Shore A hardness. Turbine blades have both spanwise and chordwise flexibility. An AR of 2.21 is used since an AR of 2.21 resulted in higher values of C_p.

Flow imaging results demonstrate that increased spanwise and chordwise blade flexibility improves self-start, ventilation, and cavitation during turbine operation. At low flow speeds, a flexible (75–85 Shore A hardness) blade turbine starts to rotate and generates electricity earlier than the less flexible one with 85–95 Shore A hardness. When both turbines are rotating at higher flow speeds, the turbine with stiffer blades can be considered more efficient since it rotates with a higher rotation speed than the turbine with flexible blades. The higher the rotation speed, the higher the C_p values. Thus, the turbine with 85–95 Shore A hardness blades will generate more power.

In summary, blade flexibility improves the issues of self-start, cavitation, and ventilation experienced during fixed-pitch Darriues turbine operation, however, it negatively impacts its performance at high flow speeds.

Conflict of Interest

There is no conflict of interest. This research did not receive any specific grant from funding agencies in the public, commercial, or not-for-profit sectors. The views and opinions expressed herein are those of the author and do not purport to state or reflect the position of the United States Government or any agency thereof, including the United States Military Academy, the Department of the Army, or the Department of Defense.

Data Availability Statement

The authors attest that all data for this study are included in the paper.

Nomenclature

A = swept area of the turbine (m^2)
C = chord length of the blade (mm)
H = height of the turbine (mm)
N = number of blades
R = radius of the turbine (mm)
T = torque produced by turbine (N-m)
U = freestream velocity (m/s)
C_p = coefficient of performance
AR = aspect ratio
Re = Reynolds number
λ = tip speed ratio
ρ = density (kg/m^3)
σ = solidity
ω = angular velocity (rad/s)

References

[1] Anyi, M., 2013, "Water Current Energy for Remote Community: Design and Testing of a Clog-Free Horizontal Axis Hydrokinetic Turbine System," Ph.D. thesis, The University of South Australia.
[2] Kirke, B., and Lazauskas, L., 2008, "Variable Pitch Darrieus Water Turbines," J. Fluid Sci. Technol., **3**(3), pp. 430–438.
[3] SHP, 2023, *Smart Hydro Power*, Smart Hydro Power, Munich, Germany. https://www.smart-hydro.de/decentralized-rural-electrification-projects-worldwide/germany-grid-connected-turbine/#project. Accessed July 24, 2023.
[4] Forbush, D., Polagye, B., Thomson, J., Kilcher, L., Donegan, J., and McEntee, J., 2016, "Performance Characterization of a Cross-Flow Hydrokinetic Turbine in Sheared Inflow," Int. Mar. Energy J., **16**, pp. 150–161.
[5] Gunawan, B., Roberts, J., and Neary, V., 2015, "Hydrodynamic Effects of Hydrokinetic Turbine Deployment in an Irrigation Canal," Proceedings of the 3rd Marine Energy Technology Symposium, METS2015, Washington, DC, Apr. 27–29.
[6] Neary, V., Fontaine, A., Bachant, P., Wosnik, M., Michelen, C., Meyer, R., Gunawan, B., and Straka, W., 2013, "US Department of Energy (DOE) National Lab Activities in Marine Hydrokinetics: Scaled Model Testing of DOE Reference Turbines," Proceedings of European Wave and Tidal Energy Conference EWTEC, Aalborg, Denmark, July 24.
[7] Ismail, A. R., and Batalha, T. P., 2015, "A Comparative Study on River Hydrokinetic Turbines Blade Profiles," Int. J. Eng. Res. Appl., **5**(5), pp. 1–10.
[8] Hashem, I., and Mohamed, M. H., 2018, "Aerodynamic Performance Enhancements of H-Rotor Darrieus Wind Turbine," Elsevier Energy, **142**, pp. 531–545.
[9] Phommachanh, S., Shinnosuke, O., Sutikno, P., and Soewono, A., 2013, "Simulation and PIV Experiment of the Ducted Water Current Turbine and Extremely Low Head Helical Turbine," ASEAN Eng. J., **3**(2), pp. 54–69.
[10] Kaprawi, S., Santoso, D., and Sipahutar, R., 2015, "Performance of Combined Water Turbine Darrieus-Savonius With Two Stage Savonius Buckets and Single Deflector," Int. J. Renew. Energy Res., **5**(1), pp. 217–221.
[11] Hantoro, R., Utama, I. K. A. P., Arief, I. S., Ismail, A., and Manggala, S. W., 2018, "Innovation in Vertical Axis Hydrokinetic Turbine—Straight Blade Cascaded (VAHT-SBC) Design and Testing for Low Current Speed Power Generation," J. Phys.: Conf. Ser., **1022**(1), p. 012023.
[12] Coiro, D. P., Nicolosi, F., De Marco, A., Melone, S., and Montella, F., 2004, "Dynamic Behaviour of a Patented KOBOLD Tidal Current Turbine: Numerical and Experimental Aspects," 4th International Conference on Advanced Engineering Design, Glasgow, UK, Sept. 5–8.
[13] Kirke, B., 2016, "Tests on Two Small Variable Pitch Cross Flow Hydrokinetic Turbines," Energy Sustain. Dev., **31**, pp. 185–193.
[14] Liu, W., and Xiao, Q., 2015, "Investigation on Darrieus Type Straight Blade Vertical Axis Wind Turbine With Flexible Blade," Ocean Eng., **110**, pp. 339–356.
[15] Butbul, J., MacPhee, D., and Beyene, A., 2015, "The Impact of Inertial Forces on Morphing Wind Turbine Blade in Vertical Axis Configuration," Energy Convers. Manage., **91**, pp. 54–62.
[16] Rivera, M., Shook, D., and Foust, E. C., 2020, "Experimental and Numerical Investigation Into Vertical Axis Water Turbine Self-Starting Phenomenon," ASME 2020 International Mechanical Engineering Congress and Exposition, Virtual, Nov. 15–19.